Original Article

Osteogenic differentiation of human mesenchymal stem cells promotes mineralization within a biodegradable peptide hydrogel

Journal of Tissue Engineering
Volume 7: 1–15

DOI: 10.1177/2041731416649789
tej.sagepub.com
SAGE

Luis A Castillo Diaz[1,2], Mohamed Elsawy[2], Alberto Saiani[2,3], Julie E Gough[3] and Aline F Miller[1,2]

Abstract

An attractive strategy for the regeneration of tissues has been the use of extracellular matrix analogous biomaterials. Peptide-based fibrillar hydrogels have been shown to mimic the structure of extracellular matrix offering cells a niche to undertake their physiological functions. In this study, the capability of an ionic-complementary peptide FEFEFKFK (F, E, and K are phenylalanine, glutamic acid, and lysine, respectively) hydrogel to host human mesenchymal stem cells in three dimensions and induce their osteogenic differentiation is demonstrated. Assays showed sustained cell viability and proliferation throughout the hydrogel over 12 days of culture and these human mesenchymal stem cells differentiated into osteoblasts simply upon addition of osteogenic stimulation. Differentiated osteoblasts synthesized key bone proteins, including collagen-I (Col-I), osteocalcin, and alkaline phosphatase. Moreover, mineralization occurred within the hydrogel. The peptide hydrogel is a naturally biodegradable material as shown by oscillatory rheology and reversed-phase high-performance liquid chromatography, where both viscoelastic properties and the degradation of the hydrogel were monitored over time, respectively. These findings demonstrate that a biodegradable octapeptide hydrogel can host and induce the differentiation of stem cells and has the potential for the regeneration of hard tissues such as alveolar bone.

Keywords

Peptide hydrogel, human mesenchymal stem cells, osteogenic differentiation, bone mineralization, bone regeneration, tissue engineering

Received: 11 January 2016; accepted: 20 April 2016

Introduction

Bone is the major structural and supportive tissue in the body, but can be compromised by degenerative diseases or trauma.[1,2] It is understandable, therefore, that research into developing and optimizing the process of bone regeneration is intense and remains of great interest. It is known that such regeneration involves a complex series of biological events of bone induction and conduction, where a number of different healthy cells or tissues lend themselves to restore lost or damaged osseous tissues. This becomes a serious challenge within the field of regenerative medicine where there are either large or small quantities of missing tissue.[1–3] One example of this is in periodontitis, which is an oral pathology that induces

[1]School of Chemical Engineering and Analytical Science, The University of Manchester, Manchester, UK
[2]Manchester Institute of Biotechnology, The University of Manchester, Manchester, UK
[3]The School of Materials, The University of Manchester, Manchester, UK

Corresponding authors:
Aline F Miller, Manchester Institute of Biotechnology, The University of Manchester, 131 Princess Street, Manchester M1 7DN, UK.
Email: aline.miller@manchester.ac.uk

Julie E Gough, The School of Materials, The University of Manchester, Manchester M13 9PL, UK.
Email: J.Gough@manchester.ac.uk

the degradation of alveolar bone.[2,4] Currently, bone grafting is the "gold standard" method used to tackle the resorption of alveolar bone;[5] nevertheless, it does not achieve effective bone regeneration.[6] Additional concerns with this methodology include high cost and the high risks associated with a surgical procedure.[7]

Over the past few years, the potential of using human mesenchymal stem cells (hMSCs) to regenerate different tissue types has been highlighted due to the cells' inherent capability to commit into different types of mature cells such as osteoblasts or chondrocytes, among others.[8,9] The differentiation of hMSCs into bone-forming cells has also been reported, where three-dimensional (3D) scaffolds have been used to host the cells and subsequently induce and control differentiation via several different approaches, including tuning the matrix stiffness,[10] incorporating growth factors,[11] combining growth factors with low-power laser photo activation,[12] heat shock stimuli,[13] or using strontium.[14] Several different types of 3D hydrogels have been reported in the literature, including both natural and synthetic systems. Examples of natural hydrogels include collagen, alginate, hyaluronic acid, or Matrigel.[15,16] These materials inherently contain active biomolecules and offer good biocompatibility, but control of their components (batch-to-batch variability) makes it difficult to define the cause of any cellular response.[16] On the other hand, synthetic biomaterials such as poly(ethylene glycol) (PEG) and peptide-based systems overcome these issues, since these materials are made of well-known components providing a minimalistic approach to the culture of cells.[17,18] Furthermore, the mechanical properties of synthetic gels are easily tunable offering an attractive route to direct the cellular response.[19–21] One limitation of these synthetic materials is that they lack bioactive molecules; however, these can be easily incorporated post-synthesis.[16] Peptide hydrogels are highly versatile, their self-assembly can be controlled from the bottom-up to form secondary structures such as α-helixes or β-sheets, for example, which self-assemble to form fibrils or fibers that subsequently entangle to form a self-supporting structure that mimics the extracellular matrix (ECM).[22,23] With the modular peptide-based systems, the solution to gel transition, the fiber, and gel morphology and consequently the resulting mechanical properties of the 3D hydrogel can be tuned easily by peptide design or varying peptide concentration, pH, ionic strength, and/or temperature.[22,23] Moreover, such peptide hydrogels are inherently biocompatible and biodegradable, and as a consequence, they have found a wide variety of applications, including drug delivery, cell culture, tissue engineering, biosensors, and supports for biocatalysts.[18] Furthermore, the translation of these soft materials into applications is starting to become a reality with the advent of routine procedures for peptide synthesis and purification on both the lab and industrial scale. This makes them easily accessible, at a reasonable cost.

Despite their numerous advantages, these peptide hydrogels have only been used in a few studies for the culture and controlled differentiation of mesenchymal stem cells (MSCs) for bone regeneration.[24–26] One example is from Anderson et al. where they incorporated the ECM moieties RGDS (arginine-glycine-aspartic acid-serine) and DGEA (aspartic acid-glycine-glutamic acid-alanine) to the end of a self-assembling peptide amphiphile ($CH_3(CH_2)_{14}$CONH-GTALIGQ—where G, T, A, L, I, G and Q are glycine, threonine, alanine, leucine, isoleucine, glycine, and glutamine, respectively). They used the nanofibrillar hydrogels to induce differentiation of hMSCs into osteoblasts by culturing under osteogenic stimulation. They went on to show that the differentiated cells were able to synthesize bone in vitro.[24]

Self-assembling peptides have also been used to create composite materials in an attempt to control the differentiation of hMSCs. For example, the RADA16 peptide (AcN-RADAADARADARADA-$CONH_2$) has been combined with a collagen sponge, and the hybrid construct induced the differentiation of hMSCs. Once the composite containing undifferentiated cells was transferred in vivo, alveolar bone mass was significantly increased, and at the same time, the population of osteoclasts (bone-resorbing cells) was downregulated. Authors hypothesized that hMSCs might have the ability to shift the pro-inflammatory macrophage program into an anti-inflammatory state, which subsequently aided the formation of bone.[25] The same peptide was also mixed with hydroxyapatite (HA), and Matsumoto et al.[26] demonstrated that this composite provided a 3D niche with good stiffness and osteoinductive properties that led to the osteogenic differentiation of murine MSCs in vivo. Thermal stimulation has also proved successful in the differentiation of stem cells, where hMSCs within the RADA16-I hydrogel deposited calcium and expressed several key bone markers only after being induced by a change in temperature.[13]

In the aforementioned approaches, generally long peptide sequences that require decoration with additional ECM signals are needed to induce MSC differentiation. In this article, we present a simplified approach where we use a cost-effective ionic-complementary octapeptide-based hydrogel, FEFEFKFK, where F, E, and K are phenylalanine, glutamic acid, and lysine, respectively. This builds on our previous work where we have shown that this ionic-complementary peptide self-assembles into β-sheet-rich fibers that entangle to form a 3D self-supporting matrix with controllable mechanical properties (Figure 1(c)).[20,27,28] We have also shown that this hydrogel can support the culture of osteoblast cells and promote mineralization under osteogenic stimulation.[29] Here, we explore the capability of the FEFEFKFK peptide hydrogel to support the 3D culture of hMSCs and induce the hMSCs' commitment into bone-forming cells. In doing this, we are demonstrating its potential for bone tissue engineering applications.

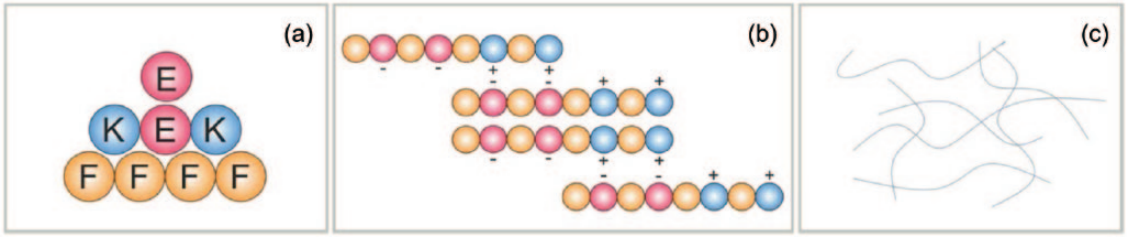

Figure 1. Schematic representation of the FEFEFKFK peptide self-assembly where hydrophobic phenylalanine (F), hydrophilic and negatively charged glutamic acid (E), and hydrophilic and positively charged lysine (K) are red, orange, and blue, respectively: (a) as building blocks, (b) as amino acids in the octapeptide associating via electrostatic interactions to form β-sheet secondary structures, and (c) form elongated fibers through non-covalent interactions, which in turn are capable of entangling into a nano-fibrous network.

Experimental

Materials and reagents

FEFEFKFK peptide>95% purity was purchased from Biomatik Corporation, Cambridge, ON, Canada. Primary hMSCs, Osteoimage™ Mineralization Assay, growth, and osteogenic cell culture medium were purchased from Lonza Walkersville Inc., Basel, Switzerland. Trypsin/ethylenediaminetetraacetic acid (EDTA), DAPI-ProLong Antifade Reagent, Alexa Fluor 488 phalloidin, rhodamine phalloidin, live/dead assay, PicoGreen Assay, and human osteocalcin (OCN) ELISA kit were purchased from Osteocalcin ELISA: Life technologies, Warrington, UK. Cell culture inserts were purchased from ThinCert™ Greiner Bio-One Limited, Stonehouse, UK. The hMSCs characterization kit was purchased from hMSCs characterisation kit: Merck Millipore Limited, Consett, UK. Secondary antibody (sAb) anti-mouse IgG Atto 594 and SIGMAFAST™ p-Nitrophenyl phosphate (p-NPP) tablets, N1891-50SET were purchased from Secondary Ab, SIGMAFAST p-Nitrophenyl phosphate, etc. Sigma-Aldrich Co. Ltd. Haverhill, UK. Rabbit polyclonal antibody for type I collagen (Col-I) and goat anti-rabbit IgG Alexa Fluor 594 were purchased from Abcam, UK. Total collagen assay was purchased from Total Collagen Assay: QuickZyme Biosciences. Upper Heyford, UK.

Methods

Hydrogel preparation

FEFEFKFK peptide (>95% purity) was used to prepare a peptide solution at 2.5 wt%. The peptide powder was dissolved in 800 µL of double-distilled water (ddH_2O). The peptide solution was subsequently vortexed and centrifuged (4000 r min^{-1}), before placing in an oven at 90°C for 1 h to ensure complete dissolution. To induce gelation, 1 M NaOH (90–95 µL) and Dulbecco's phosphate-buffered saline (DPBS) (100 µL) were added. A further vortex/centrifuge (5000 r/min^{-1}) cycle was applied and the hydrogel was placed in the oven at 90°C for 12–24 h before finally being cooled at room temperature (RT) to ensure formation of a homogeneous hydrogel.

Cell culture

Primary hMSCs obtained from Lonza were isolated from a 38-year-old Caucasian male donor. Cells were grown and maintained following standard cell culture conditions in hMSCs growth medium. At 70% of confluence, cells were subcultured using trypsin/EDTA. Cell culture medium was changed every 4 days.

3D cell culture within the FEFEFKFK hydrogel

Weak hydrogels were sterilized by ultraviolet (UV) radiation for 35 min before seeding the very viscous hydrogels with 1×10^6 cells. This was done by pipetting 200 µL of cell suspension containing hMSCs in growth/osteogenic medium on top of the weak hydrogel. The cell suspension was gently mixed by stirring with the pipette tip before gently pipetting up and down upon which the hydrogel increased in strength and yielded a homogeneous gel/cell suspension. A total of 300 µL of hydrogel containing 3×10^5 cells was transferred into each 12-well cell culture insert. The hydrogel was left to set for 10 min at 37°C in a 95% humidified atmosphere (20% O_2) with 5% CO_2. Fresh media changes were repeated five times at 20-min intervals to stabilize the pH of gels to physiological pH. After 24 h, a fresh media change was carried out, and subsequent media changes were undertaken every 4 days to aid cell growth within the hydrogel. For all stimulated samples, cells were treated with osteogenic media after 2 days of culture.

Cell viability

Cell viability was explored using a standard live/dead assay. Live/dead assay solution was prepared using 1.5 mL of phosphate-buffered saline (PBS) containing 2.5 µL of 4-µM ethidium homodimer-1 (EthD-1) assay solution and 1.5 µL of 2-µM calcein acetoxymethyl (AM) assay solution. The assay solution was pipetted on top of each hydrogel and then incubated under standard cell culture conditions for 20 min. The assay solution was then removed and samples were viewed under a Leica TCS SP5

confocal microscope. To determine the number of viable cells, five different confocal microphotographs (representing five different areas of hydrogel) were used to manually quantify viable cells. Cell clusters were considered as a single cell.

Cell proliferation

The hMSC proliferation was quantified using PicoGreen dsDNA Assay. Gels were rinsed twice using DPBS and then they were resuspended in 700 µL of cold lysis buffer (200-mM Tris-HCl, 20-mM EDTA/ddH_2O/1% Triton X-100) for 15 min. To ensure complete cell lysis, samples were vortexed vigorously and subjected to three freeze–thaw cycles. Thereafter, samples were resuspended, and 100 µL of gel/cell suspension was plated into dark 96 wells, where 100 µL of a working solution of Quant-iT PicoGreen reagent was added. The samples were incubated for 2–5 min at RT. Fluorescence readings were obtained in a plate reader (FLUOstar OPTIMA BMG LABTECH) at 435 nm (excitation) and 529 nm (emission). A standard curve was determined using calf thymus DNA in serial dilutions in 1% (v/v) Triton X. A blank gel was used to correct the background absorbance, and the assay was performed in triplicate.

hMSCs characterization

Stem cell characterization was carried out using immunocytochemistry (ICC). An hMSC characterization kit, from which Stro-1, Thy-1 (CD90), and CD19 markers, was used to characterize the undifferentiated state of cells either with or without osteogenic stimulation. After 2 days, stimulated samples were treated with osteogenic media. At each time point, gels were rinsed twice (5 min each) with 1× PBS. Thereafter, samples were fixed in 4% (w/v) paraformaldehyde (PFA) for 30 min at RT. Subsequently, samples were washed three times (5 min each) with 1× PBS and permeabilized using Triton X-100 at 0.1% (v/v) in DPBS for 15 min at RT. Samples were then blocked with 1% (v/v) bovine serum albumin (BSA) for at least 2 h at RT and incubated overnight at 4°C with mouse primary antibodies (pAb) anti-STRO-1, anti-THY-1 (CD90), and anti-CD19, respectively, at the ratio stipulated by the manufacturer (1:500 dilution). The next day, samples were washed twice (5 min each) with 1× PBS and twice with blocking solution. After the last wash, samples were left in the blocking solution for at least 30 min. Thereafter, samples were incubated for 2 h at RT in the dark with a sAb anti-mouse IgG Atto 594, along with Alexa Fluor 488 phalloidin to target F-actin filaments. Both sAb and phalloidin were used at ratios stipulated by the manufacturer (1:250). Samples were finally washed three times (5 min each) with 1× PBS before being mounted on glass slides using DAPI-ProLong Antifade Reagent to stain cell nuclei. Images were obtained using a Leica TCS SP5 confocal microscope. Two independent assays were performed, each in duplicate.

ICC for Col-I

Type 1 collagen production within the gel sample was examined visually using the same ICC staining procedure as for hMSCs characterization, except here a rabbit polyclonal antibody for Col-1 was used as the stain at a ratio stipulated by the manufacturer (1:250). After 24 h, samples were incubated for 2 h at RT in the dark with a goat anti-rabbit IgG Alexa Fluor 594 along with Alexa Fluor 488 phalloidin to target F-actin filaments. Both sAb and phalloidin were used at ratios stipulated by the manufacturer (1:250). The samples were mounted and confocal images obtained as before. Two independent assays were again performed in duplicate.

Quantification of proteins

The production of bone proteins by hMSCs was quantified using spectrophotometric assays. After 6 and 12 days of culture, cell-loaded gels were subjected to three freeze–thaw cycles to ensure cellular lysis. The osteogenic markers that were quantified included total collagen, OCN, and alkaline phosphatase (ALP). For all protein quantification experiments, cells without osteogenic stimulation were used as control, and a blank gel was used to correct for background absorbance. All experiments were normalized to cell numbers from the PicoGreen Assay and gel volume over time. Details for each assay are given below.

Total collagen

Total collagen production was determined using a total collagen assay. After resuspending and lysing, samples were vortexed and hydrolyzed over 20 h at 95°C with 100-µL 12 M HCl. Samples were subsequently diluted 1:1 in 4 M HCl, pipetted into a 96-well plate, before adding 75 µL of an assay buffer and leaving to incubate for 20 min at RT. Afterward, 75 µL of a detection reagent was added, and the sample transferred into the oven (60°C) for 1 h. Absorbance measurements were obtained at 570 nm, using a plate reader (TECAN Infinite M200). Two independent assays were undertaken in triplicate.

OCN

OCN expression was determined using a Human OCN ELISA Kit. After cellular lysis using cold distilled water, samples were vortexed and pipetted into a 96-well plate. Subsequently, a working anti-OST-HRP solution (100 µL) was added to each well, the plate covered and incubated for 2 h at RT. Each well was then rinsed three times with a

washing solution before adding 100 µL of a chromogen solution (tetramethylbenzidine) and incubating for 30 min at RT in the dark. The reaction was stopped by adding 100 µL of a stop solution (1 N HCl). Absorbance measurements were obtained within 1 h at 450 nm using a plate reader (TECAN Infinite M200). Two independent assays were performed in triplicate.

ALP

ALP activity was monitored using a colorimetric ALP and peroxidase substrate detection system. The cell lysate (20 µL) was added to transparent 96-well plates together with 200 µL of p-NPP solution (1 mg mL^{-1} p-NPP, 0.2-M Tris buffer in 5-mL ddH_2O) SIGMAFAST p-NPP tablets, N1891-50SET. The reaction was stopped with 3 M NaOH. The absorbance of samples was measured using a plate reader (LabSystems Multiskan Ascent) at 405 nm every 30 s for 30 min. Two independent assays were performed in triplicate.

Mineralization (HA deposition)

The extent of mineralization was determined using an Osteoimage Mineralization Assay. After each culture time point, the gels were washed with 1× PBS before being fixed with 4% (w/v) PFA for 20 min at RT. Samples were subsequently washed further twice (5–10 min each) with Osteoimage wash buffer and then incubated with 1.5-mL staining reagent, along with rhodamine phalloidin (1:250 dilution) to target F-actin filaments at RT in the dark for 30 min. After incubation, gels were washed three times (5 min each) with wash buffer before mounting the samples on glass slides using a DAPI-ProLong Antifade Reagent to stain the cell nucleus. Images were obtained using a Leica TCS SP5 confocal microscope. To quantify the extent of mineralization, washed samples were resuspended in 700-µL wash buffer and their fluorescence determined in a fluorescent plate reader at a 492/520 nm ratio. Two independent assays were performed, again in triplicate.

Hydrogel volume tracking

The percentage volume of FEFEFKFK peptide hydrogel (25 mg mL^{-1}, 20 mM) with and without cells was qualitatively and quantitatively monitored over time under cell culture conditions. Photographs of hydrogels were taken using a Canon EOS 1100D camera. To quantify the percentage of hydrogel volume, 300 µL of hydrogel was plated into each cell culture insert and this gel was considered as 100% hydrogel volume. At days 1, 6, and 12, the cell culture medium was removed completely from each hydrogel. Thereafter, 700 µL of distilled water was added to each hydrogel, which was broken down by pipetting up and down. The resuspended solution was transferred into a 15-mL Falcon tube, and the total volume was measured using a standard micropipette. Finally, the difference in volume obtained from each sample was subtracted from the 100% gel volume. Two independent measurements were carried out in duplicate.

Oscillatory rheology

The viscoelastic properties of the hydrogel (25 mg mL^{-1}, 20 mM) were undertaken using an AR-G2 rheometer equipped with a 20-mm parallel plate. Hydrogels with and without cells were run in parallel. A total of 150 µL of hydrogel sample was loaded onto the bottom plate, and the upper plate was lowered until it reached a 250 µm gap. Thereafter, the sample was left for 10 min to equilibrate before recording the elastic (G′) and viscous (G″) moduli as function of strain (0.04%–40.00%) at 1 Hz and oscillatory frequency (0.01–15 Hz) at 0.2% strain. Samples were maintained at physiological temperature (37°C) using a Peltier stage, and a solvent trap was used to minimize sample dehydration. All measurements were carried out in triplicate.

Hydrogel proteolytic degradability

FEFEFKFK peptide hydrogel (25 mg mL^{-1}, 20 mM) was incubated with and without hMSCs using cell culture media, both in the presence and absence of 10% fetal bovine serum (FBS) following the procedures outlined earlier. After incubation for 1, 6, and 12 days, the gel was broken down by dilution to 1 mg mL^{-1} in 1% trifluoroacetic acid (TFA) in water/acetonitrile (50/50 v/v). The peptide solutions were injected on the reversed-phase high-performance liquid chromatography (RP-HPLC) column Phenomenex Jupiter 4-µm Proteo column 90 Å (250 × 4.66 mm). An elution gradient was used with a flow rate of 1 mL min^{-1} that went from 90% solvent A (0.05% TFA in H_2O)/10% solvent B (0.05% TFA in CH_3CN) to 30% solvent A/70% solvent B in 45 min. The peptide stability was expressed as a percentage of intact FEFEFKFK peptide using the following equation

$$\%\ \text{intact peptide} = \left(\frac{\text{AUC t}}{\text{AUC t}_0} \right) \times 100$$

where, AUC t and t_0 are the area under the HPLC curve from the FEFEFKFK peptide peak as calculated by Chromeleon software at the sampling time point and day 0, respectively. At least two repeat experiments were undertaken.

Statistical analysis

Statistical significance in PicoGreen, total collagen, ALP activity, OCN quantification assays, hydrogel volume, mechanical properties, and proteolysis was determined using one-way analysis of variance (ANOVA) followed by post-hoc comparisons (Tukey's method).

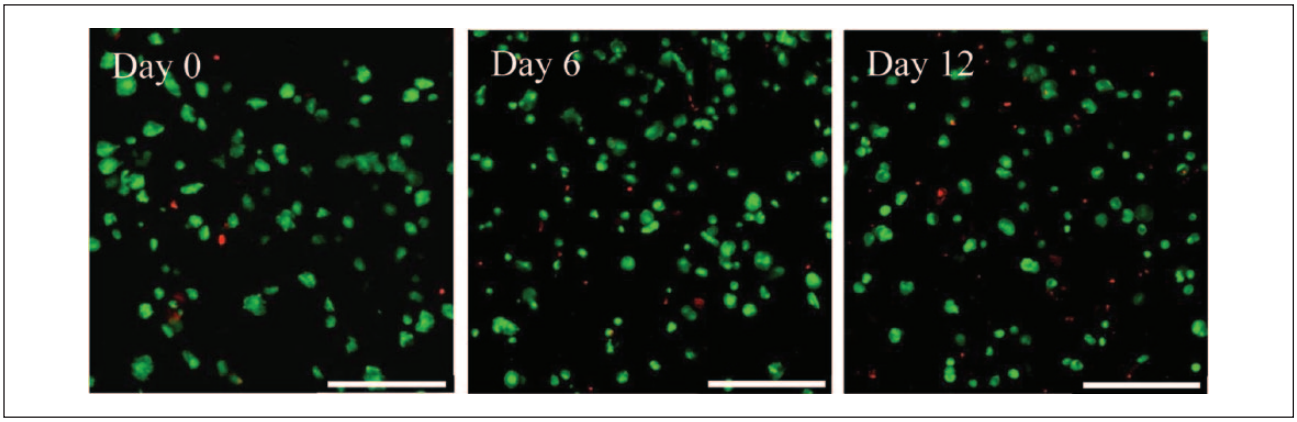

Figure 2. Live/dead assay showing viable (green) and non-viable (red) hMSCs within the FEFEFKFK gel over 12 days of cell culture. Magnification = 20×. Scale bars = 250 µm.

Results and discussion

Cell viability, morphology, and proliferation

The first step in this work was to confirm the capability of the FEFEFKFK peptide hydrogel to support the viability and proliferation of hMSCs when incorporated within the peptide hydrogel in 3D. Cell viability was therefore assessed initially using a live/dead assay over a period of 12 days of culture. It is clear from the confocal images shown in Figure 2 that the majority of hMSCs remained viable over 12 days of culture within the gel, with only a few dead cells being present. Therefore, the gel provided an adequate niche for cell survival. Cell viability was subsequently quantified (Figure 3), and it was found that the number of living cells increased significantly during the first 6 days and then decreased slightly over the remaining days of culture. This decrease could be due to cells undergoing cell senescence or death. The number of dead cells in Figure 2 does not increase over time in culture and as will be shown later, the cells remain functional and positive effects on the markers studied were observed, so senescence is not likely. Such viability data are consistent with what we have previously reported for human osteoblasts[29] and bovine chondrocytes[19] when encapsulated throughout the FEFEFKFK hydrogel. This is also in agreement with the results reported using other synthetic scaffolds, which include peptide- and polymer-based hydrogels such as RADA and PEG gels, where rat neural stem cells and hMSCs showed a steady viability within such gels at similar cell culture time.[13,30]

Confocal microscopy imaging (Figure 2) also shows that most cells acquired a round/ovoid morphology during the first day of culture. As time progressed further (days 6 and 12), cells acquired a definite round shape. This was expected, as cells typically remain rounded when embedded within a 3D niche that contains no adhesion sites. Optical microscopy was also used to confirm cell morphology (Figure 4(a)) and the data obtained corroborated the conclusions from confocal imaging. Interestingly, hMSCs were also cultured in 2D on top of the tissue culture plastic (TCP) where they acquired a typical spindle morphology and these became wider under osteogenic stimulation (Figure 4(b)), as is typical for flattened surfaces.[9]

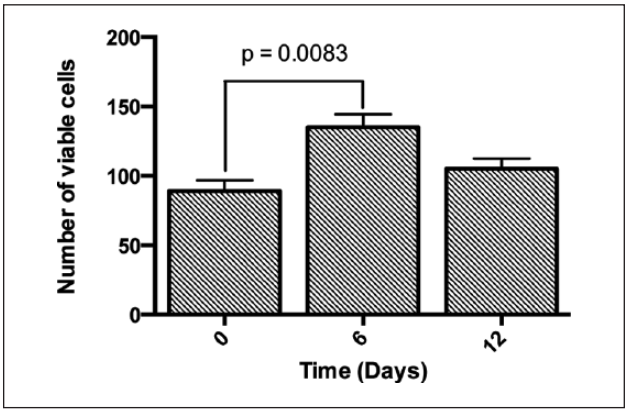

Figure 3. Quantification of viable cells encapsulated within the FEFEFKFK gel over 12 days of culture by manually counting viable cells in five different confocal microphotographs (n = 3).

The extent of cell proliferation within the FEFEFKFK hydrogels with no stimulation was subsequently quantified using the PicoGreen Assay and the results are given in Figure 5. It is clear that cell numbers were sustained, indicating that cells could be maintained within the hydrogel over 12 days of culture. There was a slight drop in number between days 6 and 12, which matches with the viability trend at the same time point. Moving through these time points, the rate of overall cell proliferation is likely to be sufficient to lead to bone formation, if and when osteogenic differentiation is induced within the gel. This is because it is known that the rate of human osteoblast population in native bone is relatively lower and ~60%–90% of the osteoblast population dies by apoptosis after synthesizing new osteoid.[31] Such osteoblast proliferative behavior

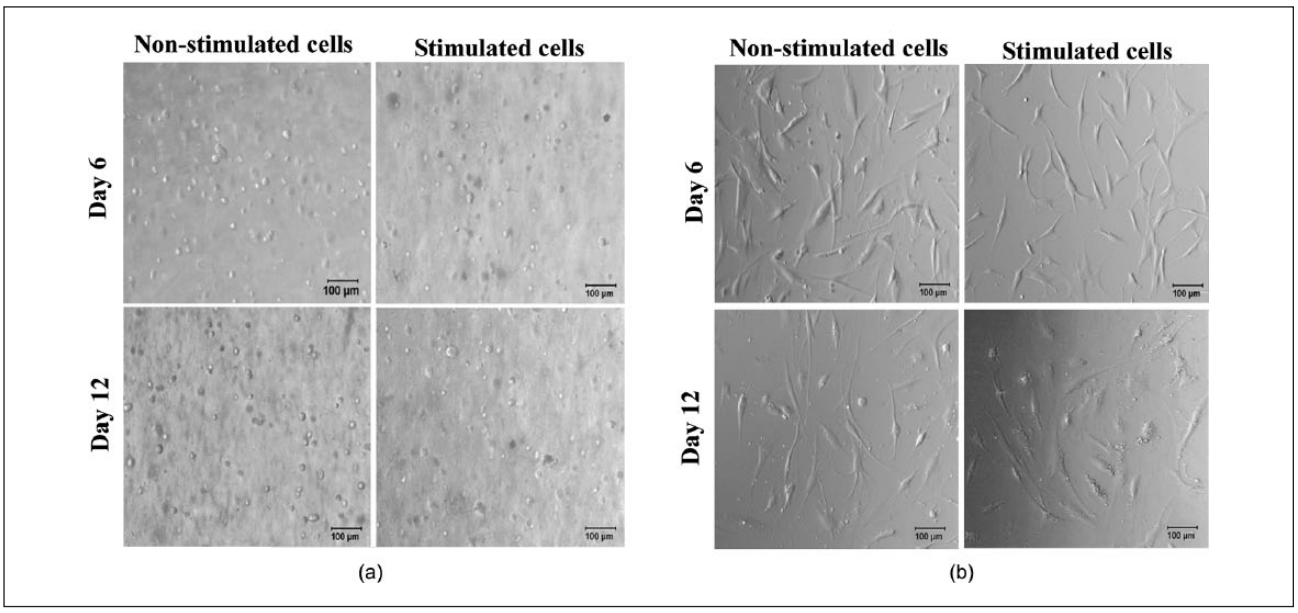

Figure 4. Optical microscopy images showing the morphology of hMSCs when (a) encapsulated within the FEFEFKFK hydrogels and (b) placed on TCP, with and without osteogenic induction over 12 days of culture. Magnification = 10×. Scale bar = 100 µm.

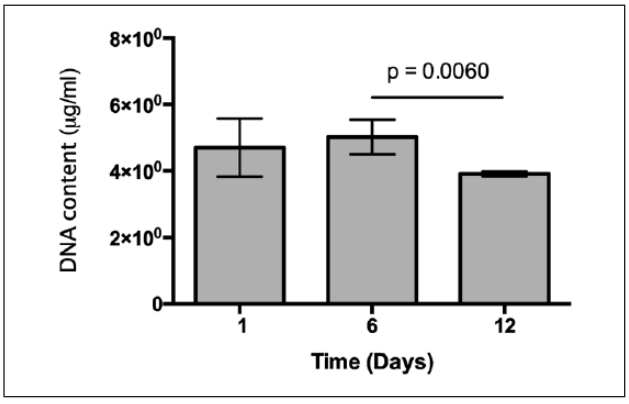

Figure 5. DNA content normalized to hydrogel volume over 12 days of culture (n = 3) under non-stimulated conditions.

observed here is commensurate with similar systems in the literature.[32,33]

MSCs characterization

To demonstrate that the hMSCs seeded into the peptide hydrogels were fully undifferentiated initially and remained so over time, the plasticity of the cells within the hydrogels was determined using ICC staining for two well-known positive hMSCs markers; stro-1 and CD90 (thy-1), as well as staining for CD19 as the negative control. This was done for cells embedded within the hydrogel, both with and without osteogenic stimulation, and all images obtained were compared to the non-sAb controls to rule out the staining observed being due to non-specific staining. Confocal images shown in Figure 6(a) and (b) revealed the presence of both Stro-1 and Thy-1, respectively, over 12 days of culture in growth medium only, that is, non-stimulated conditions. This confirmed the stem cell characteristic of cells within the gel. Interestingly, the expression of the positive stem cell markers decreased slightly at day 12. This stem cell marker behavior has been reported in the literature, where subcultured stem cells tend to lose the expression of their stemness markers over time, either with or without osteogenic stimuli.[34,35] Likewise, the loss of the expression of Thy-1 in hMSCs cultured under chondrogenic stimuli has been reported using different substrates including alginate gels.[36] When stem cells within FEFEFKFK hydrogels were stimulated to differentiate using osteogenic media, the positive "stem cell" markers were found to be expressed at a much reduced level in comparison to observed cells cultured with growth media, a result that matches with other studies reported in the literature.[34,35] In support of the characterization of the hMSCs, there was no evidence of the presence of the negative control CD19 within the hydrogel (Figure 7) both with and without osteogenic stimulation. This was expected, as it is a marker exclusively expressed by B lymphocytes. In summary, these findings suggest that stem cells may shift from their undifferentiated state into a differentiated state in the presence of the osteogenic medium.

ECM production

To confirm the possible differentiation of hMSCs within the hydrogel matrix, the expression of Col-1 was monitored over time in culture by staining for the prototypical

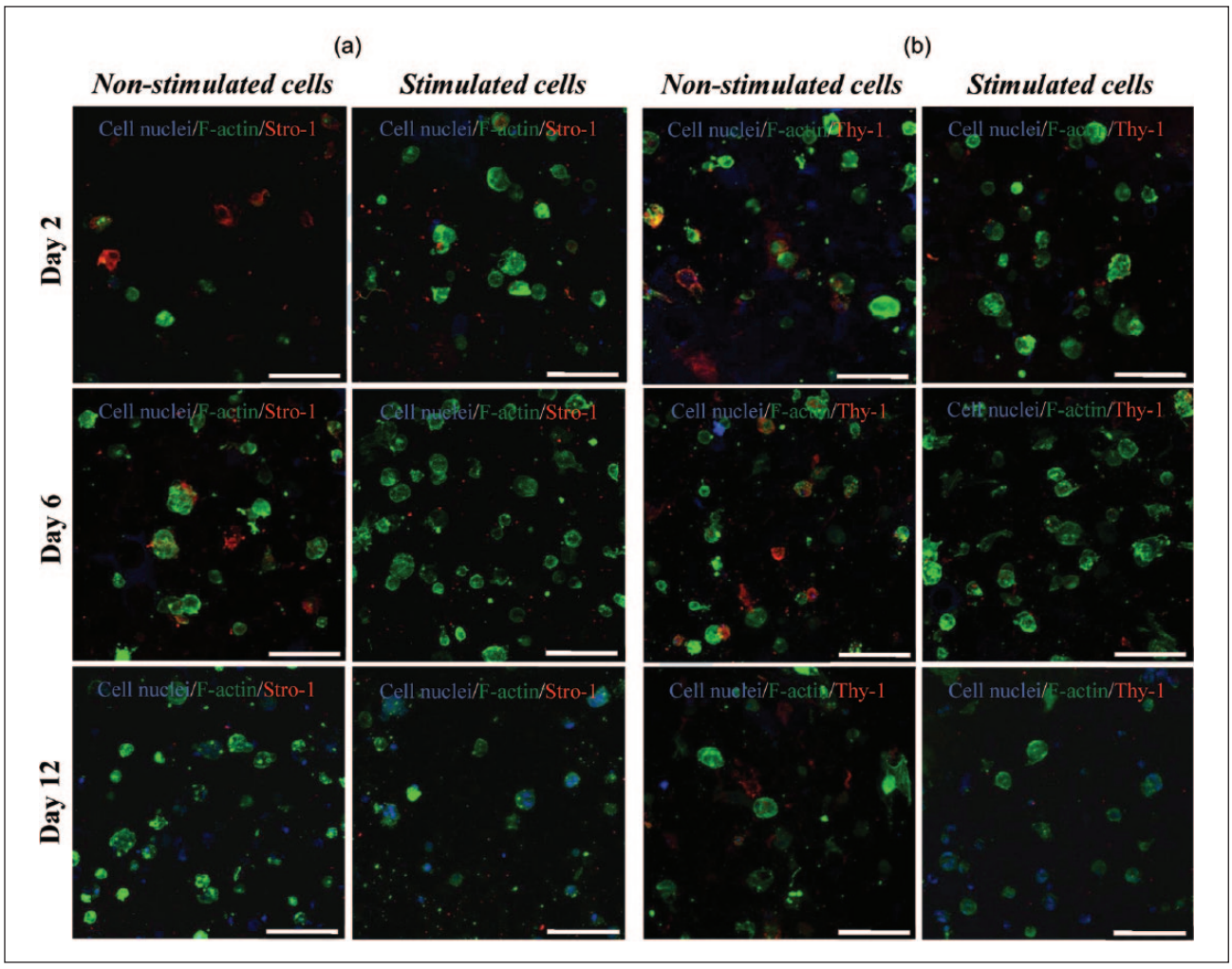

Figure 6. (a) ICC staining for Stro-1 (red) and (b) Thy-1 (red) within the FEFEFKFK hydrogel, with and without osteogenic stimuli over 12 days of culture (n = 2). Cell nuclei and F-actin are stained in blue and green, respectively, to characterize cell architecture. Magnification = 40×. Scale bar = 100 µm.

marker using ICC. The expression of Col-1 is a good parameter of cell differentiation in this case, as it is the major component of organic bone matrix (~90%).[1] As a first step, samples were imaged in the absence of the Col-1 antibody, and images taken did not exhibit any fluorescent signal, thus confirming the hydrogel and cells did not display any unspecific or auto-fluorescence. Confocal imaging of samples with the Col-1 antibody revealed hints of Col-1 inside the hydrogel at days 6 and 12 under non-stimulating conditions as evidenced by the red staining (Figure 8). Under osteogenic stimulating conditions, some Col-1 staining was also observed at day 6 of culture; however, this increased significantly at 12 days of culture suggesting the cells committed into an increasing differentiated profile over extended time in culture but not necessarily toward an osteoblastic lineage. Furthermore, it is clear from the confocal images in Figure 8 that the stimulated cells embedded within the FEFEFKFK matrix were also able to deposit the synthesized collagen in the surrounding gel, not just close to the cells. This behavior is also reminiscent of our previous work where human osteoblasts were cultured in 3D within the same hydrogel.[29] The total collagen synthesized by stem cells was subsequently quantified using a spectrophotometric assay. The normalized total collagen production observed during these assays is shown in Figure 9(a) for both the non-stimulated and osteogenically stimulated cells. The data corroborate the trends observed in the ICC staining experiments, where collagen was produced in the stimulated conditions and the quantity of collagen increased over prolonged time in culture. This pattern in collagen synthesis is in good agreement with data reported for the differentiation of MSCs into osteoblast cells in other matrices such as PEG[30] and honeycomb collagen scaffold.[37]

The production of Col-1 is, however, not exclusive to osteoblast cells, therefore, we also quantified the production and activity of two key bone proteins involved in bone formation and mineralization: OCN and ALP. Data normalized

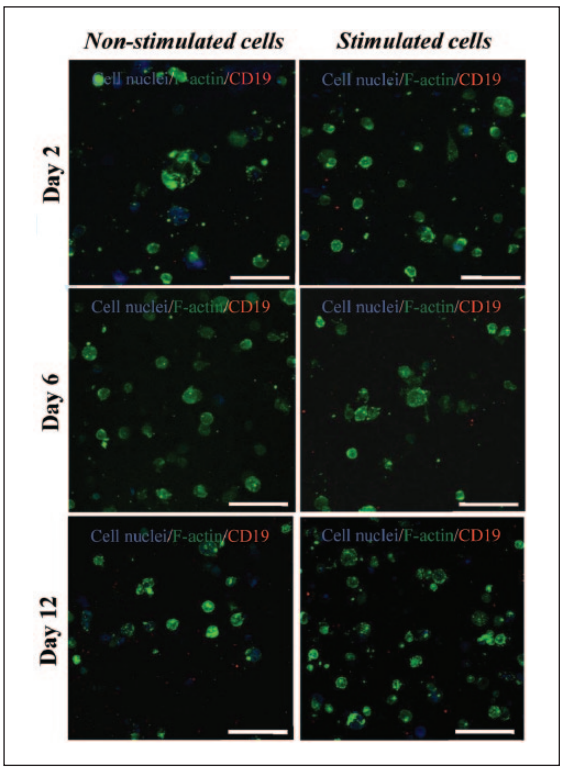

Figure 7. ICC staining for CD19 (red) within the FEFEFKFK gel with and without osteogenic stimuli over 12 days of culture (n = 2). Cell nuclei and F-actin are stained in blue and green, respectively, to determine the cell architecture. Magnification = 40×. Scale bars = 100 µm.

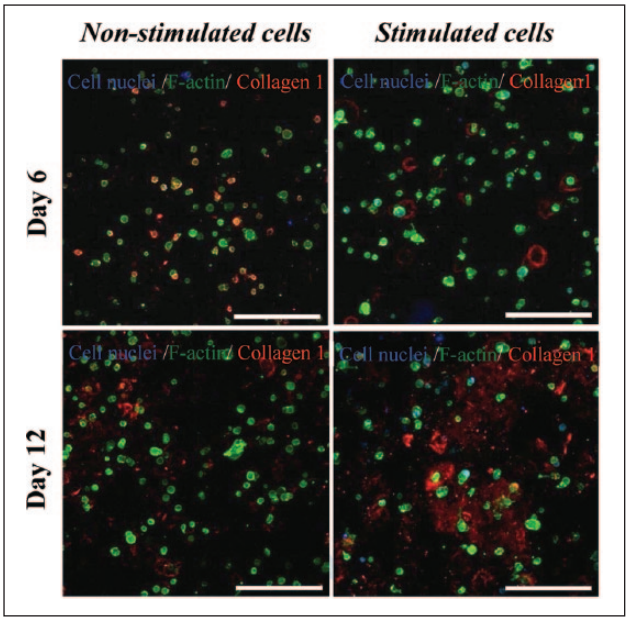

Figure 8. ICC staining for type I collagen (red) within the FEFEFKFK gel with and without osteogenic stimuli over 12 days of culture (n = 2). Cell nuclei and F-actin are stained in blue and green, respectively, to determine the cell architecture. Magnification = 20×. Scale bars = 250 µm.

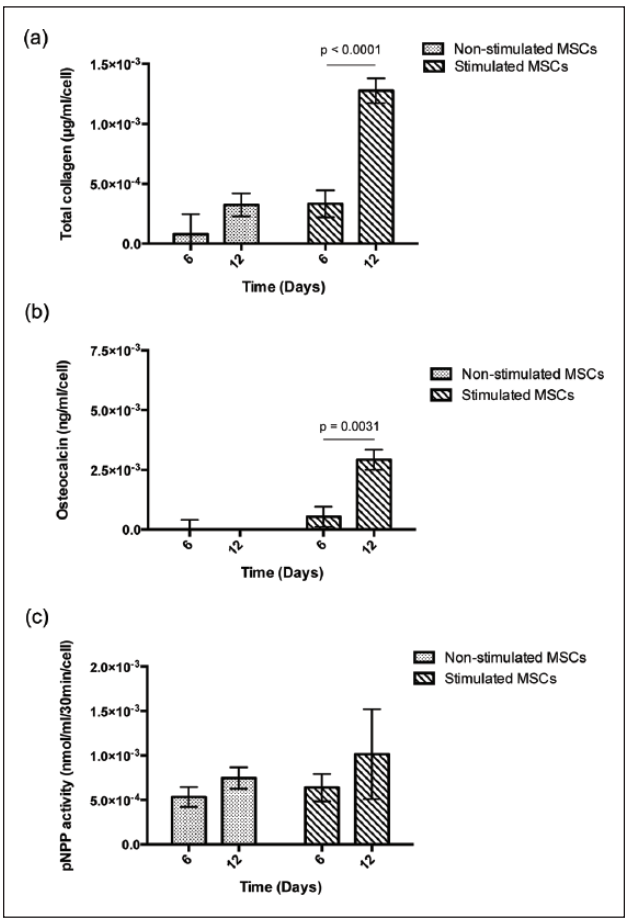

Figure 9. Quantification of bone protein production by hMSCs: (a) total collagen production, (b) osteocalcin production, and (c) alkaline phosphatase activity, with and without osteogenic stimuli within the hydrogel over 12 days of culture. Data are reported as mean ± standard deviation for n = 2 and are normalized against cell numbers and hydrogel volume.

to cell numbers and hydrogel volume over time for each of these are given in Figure 9(b)and (c), respectively. It is clear that the data for the presence of OCN are very similar to the production of collagen (Figure 9(a)), where the production of OCN was observed at the latest time point for the osteogenic stimulated sample. This is in good agreement with similar studies reported in the literature[24,37] and points to osteogenic differentiation of the hMSCs. Similar trends were observed for ALP activity (Figure 9(c)), although there was less of an increase between the non-stimulated and stimulated cells in this case. In the literature, the majority of studies report an increase in the presence of ALP once the osteogenic differentiation of hMSCs is induced.[13,38] It is known that the differentiation of hMSCs into osteoblasts in vitro can take between ~14 and 30 days, where cells generally proliferate during the first 7 to 14 days. Only at this point the differentiation process starts where the transcription and the expression of ALP are carried out.[13,39] Therefore,

in this study, we believe the differentiation of hMSCs and subsequent expression of ALP could have been accelerated and reached its peak over the first 12 days. This has been reported by others[13,38] and could explain the lack of significant increase in ALP activity between days 6 and 12 under osteogenic stimulation within the hydrogel. Based on these studies, any cell differentiation observed during culture could be concluded to be induced either by the environment surrounding cells (i.e. the hydrogel) or the osteogenic stimulation applied (i.e. presence of the osteogenic media), or both. Certainly, further studies are needed to determine whether the mechanical properties of gel or the 3D environment induced this acceleration of the ALP production rate.

Thus far, we have shown that the FEFEFKFK peptide hydrogel can act as a 3D support for the proliferation and differentiation of hMSCs into osteoblast cells that go on to produce key bone proteins involved in bone formation. This is greatly facilitated when the cells are stimulated by osteogenic media. The next step was to determine whether these hydrogels support mineralization under the same cell culture conditions. First, to rule out that the mineralization occurred via cell death/apoptosis inducing mechanism, we looked at the number of live/dead cells and did not see a significant number of dead cells present. Second, we monitored mineralization by introducing a staining reagent into the hydrogel that specifically binds to HA. Any binding was then detected using a fluorescent assay and compared to the control sample, which remained completely blank, where no cells were incorporated within the gel.

Confocal images of stained samples at days 6 and 12 of culture, both with and without the addition of osteogenic stimuli, are given in Figure 10(a). The presence of HA (green fluorescence staining) was apparent after 6 days of culture with osteogenic stimulation. Our findings correlate with those reported in the literature, where hMSCs differentiated under osteogenic stimulation and subsequently mineralized within polyethylene glycol diacrylate (PEGDA) hydrogels that were functionalized with the short fibronectin peptide RGD.[40,41] Although the process of bone mineralization is not fully understood yet, it is believed that apatite binds to Col-1 fibrils, which serve as a spatial framework for crystal deposition.[42] Non-collagen proteins including OCN are needed to complete this process.[43,44] Thus, we believe that HA deposits observed within the gel derived from the interaction of amorphous calcium phosphate with the bone proteins deposited by differentiated cells in the fibrillar network of the peptide hydrogel. Only a faint hint of green fluorescence is observed after 12 days of culture without the addition of osteogenic stimulation, which may be explained due to the lower or null production of bone proteins observed in the protein quantification. The amount of mineralization occurring in each case was also quantified, and it is clear from the data in Figure 10(b) that significant mineralization only occurred after prolonged time in culture under

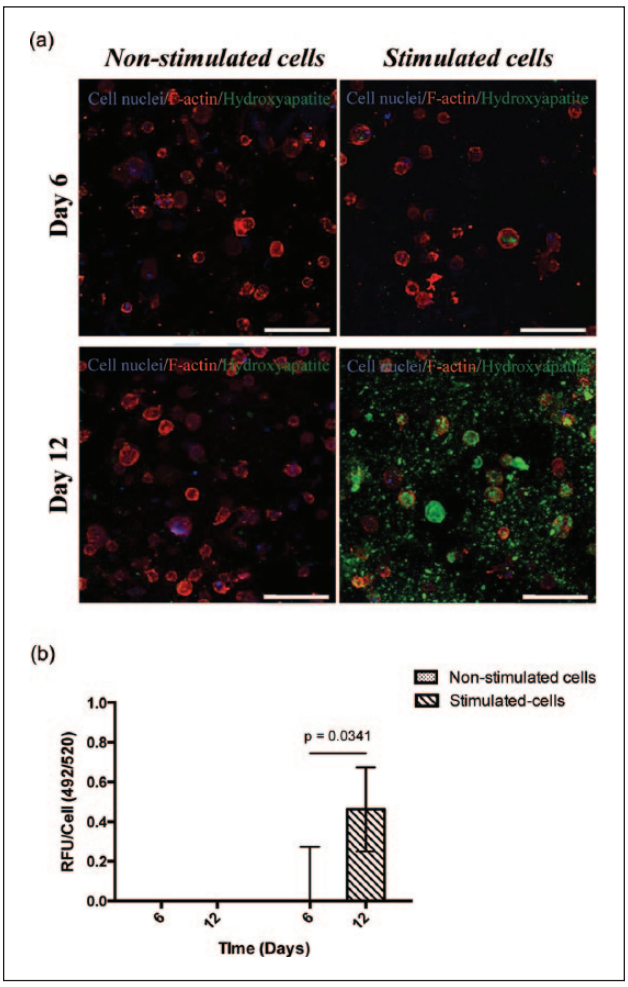

Figure 10. (a) Confocal imaging of mineralization/hydroxyapatite deposits (green) within the FEFEFKFK hydrogel, with and without osteogenic stimuli over 12 days of culture (n = 2). Cell nuclei and F-actin are stained in blue and red, respectively. Magnification = 40×. Scale bars = 100 µm. (b) Quantification of relative fluorescence units normalized to cell numbers from the PicoGreen Assay to determine mineralization within the hydrogel with and without osteogenic stimuli over 12 days of culture (n = 2).

stimulated conditions. Such behavior agrees well with the previous protein quantification work presented in Figure 9 indicating bone ECM production. This finding clearly demonstrates the suitability of the FEFEFKFK hydrogel to host hMSCs and promote their differentiation into osteoblast cells, in particular, under osteogenic stimuli. In addition, this finding is in good agreement with previous studies, where the osteogenic differentiation of murine and human stem cells has been induced in the longer RADA16 peptide sequence[45] and in a phosphate-containing PEG[46] gel, respectively, over a similar time period of 1–4 weeks of culture. The advantage of our octapeptide-based system is its short length (hence, reduced cost), it does not require the addition of ECM-functionalized peptide groups (such

as RGDS and DGEA), and also its ease of handling and injectability.

Hydrogel behavior

The 3D fibrillar network structure of the peptide hydrogels offers a protective matrix for cells, and when encapsulated, the cells can mirror the physiological functions undertaken in the body such as proliferation or ECM remodeling.[47,48] As hydrogels typically degrade progressively, they fuse with native tissues without the need to introduce additional hydrolytic elements. Herein, it is hypothesized that the physiological cell activity described earlier (proliferation, ECM remodeling, and mineralization) might influence the mechanics, and hence the inherent biodegradability of the hydrogels is studied here. In turn, we believe that the biodegradability of hydrogels may influence cellular function. Consequently, the volume and viscoelastic properties of the hydrogel were monitored as a function of time in both the presence and absence of cells. Over the course of 12 days of cell culture conditions, the FEFEFKFK peptide hydrogels (25 mg mL^{-1}, 20 mM) shrank progressively (Figure 11(a)). This was expected due to the hydrolytic effect as the surrounding media was changed continuously. In addition, enzymes present in the serum along with the natural proteolytic activity from the ECM remodeling by the cells could contribute to hydrogel shrinkage.[49,50] Interestingly, samples containing cells exhibited a more noticeable decrease in volume in comparison with control samples with no cells. This is most evident at day 12 of culture (Figure 11(a)). To monitor this further, the percentage of hydrogel volume was quantified and results are presented in Figure 11(b). It was found that both hydrogel samples decreased progressively, and a lower hydrogel volume was recovered over culture time in the presence of cells. This corroborates the visual observations and also highlights the erosion and/or biodegradability of the FEFEFKFK hydrogel. Such hydrogel erosion might initiate intracellular signaling that would lead to cell migration or downregulation of cellular activity, as the cells sense a smaller area in which they interact and survive in vitro. It should be noted that this is not necessarily occurring when cell-loaded hydrogels are transferred into the body.[51,52]

Thus far, our results suggest erosion of the hydrogels due to media changes but also an effect of enzyme-mediated activity from cells and/or serum on the biodegradability of the peptide hydrogel. Interestingly, El-Fiqi et al., reported the progressive shrinkage of collagen hydrogels and the subsequent decrease in the viscoelastic properties of such hydrogels when MSCs were cultured in 3D. They also showed that the incorporation of mesoporous bioactive glass nanoparticles (mBGns) into their hydrogels improved the mechanical properties and decreased the shrinkage of collagen hydrogels caused by the proteolytic effect derived from cells and serum.[50] To study whether

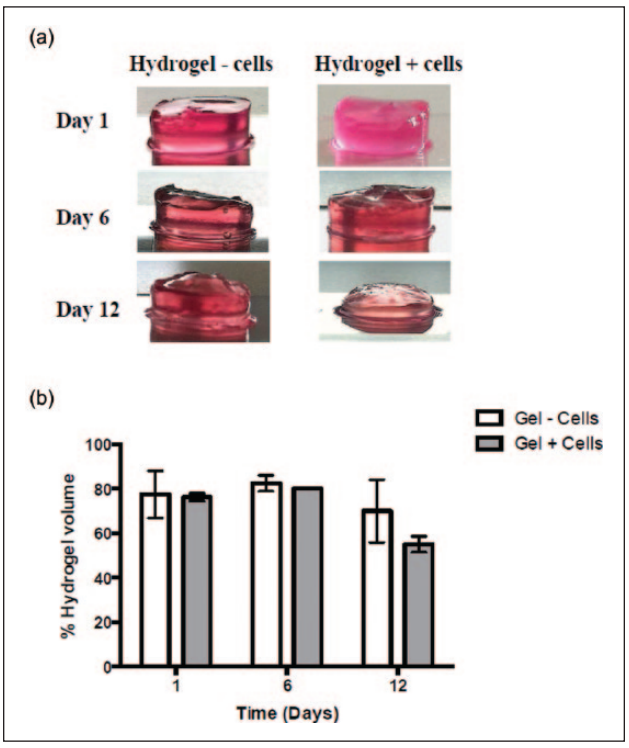

Figure 11. (a) Photographs of FEFEFKFK hydrogels over 12 days of cell culture conditions. (b) Measurement of the percentage of FEFEFKFK hydrogels volume, with and without cells over 2 weeks in cell culture conditions. Data are reported as mean ± standard deviation for n = 3.

the viscoelastic properties of the FEFEFKFK hydrogels studied here were influenced by any cellular metabolic activity, the elastic behavior of the hydrogels with and without cells was monitored as a function of time in culture. The hydrogels containing cells displayed a progressive decrease in the storage modulus, G′, which decreased from 45,000 ± 6000 Pa at day 1 to 10 ± 1 Pa at day 12 (Figure 12). The control samples exhibited a similar trend, although G′ decreased to a lesser extent from 40,000 ± 7000 Pa at day 1 to 4500 ± 1000 Pa at day 12 (Figure 12). These data match the trends observed in the hydrogel volume studies and corroborate the proposal that there is a proteolytic effect on the hydrogel degradability derived either from cells or serum, or both. Likewise, these findings are in good agreement with our observations relating to ECM remodeling by the hMSCs within gels discussed earlier and with other similar studies in the literature.[50,53] For example, Swanekamp et al. recently demonstrated that the G′ of such peptide hydrogels decreased significantly when the hydrogels were subjected to the enzymatic activity of various proteases, including α-chymotrypsin, trypsin, and proteinase K.

In parallel, the mechanical properties of the surrounding ECM may have a significant influence on cell functions including proliferation[54,55] and differentiation even in

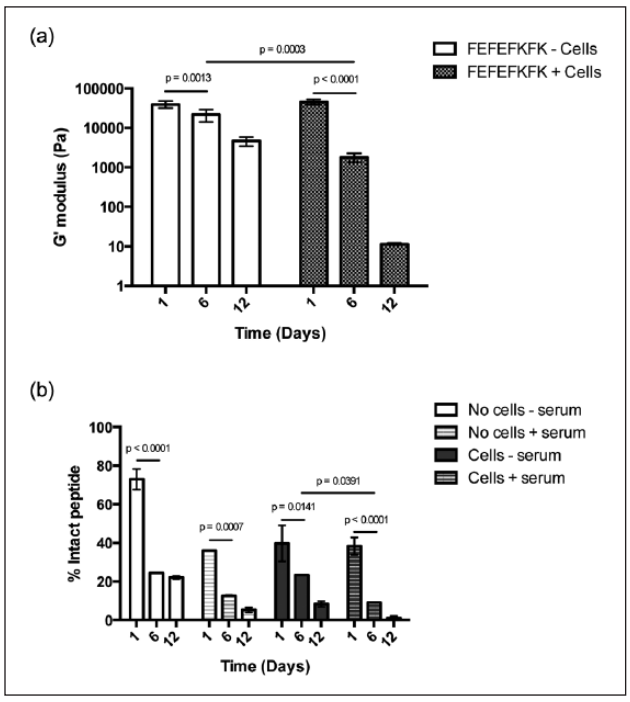

Figure 12. (a) Elastic modulus, G′, of peptide hydrogels with and without cells over 12 days of cell culture conditions. (b) Enzyme-mediated proteolytic degradation of FEFEFKFK hydrogels over 12 days of cell culture conditions. Data are reported as mean ± standard deviation for n = 3.

the absence of any osteogenic stimuli.[17,54–56] For example, hydrogel stiffness might impact cell numbers, as it has been reported that relatively stiff hydrogels with G of 20,000 Pa can induce the osteogenic differentiation of MSCs even without the use of any osteogenic supplements.[17] Once differentiated, the rate of hMSC proliferation might decrease as reported by Anderson et al.[24] The initial elastic modulus (ca. 40,000 Pa) recorded for FEFEFKFK hydrogel (20 mM) is higher in comparison with other peptide hydrogel systems used for differentiating stem cells, such as RADA-16.[57,58] The osteogenic commitment of hMSCs might potentially, therefore, be induced only by the gel stiffness here, which might explain the observed hints of ECM production without osteogenic stimuli. At this stage, we do not rule out that both the osteogenic stimulation and the mechanical properties of the gel might impact the plasticity of hMSCs and this hypothesis is the subject of an ongoing study.

Overall, the findings discussed suggest that the FEFEFKFK peptide hydrogel has a substantial effect on the hMSCs viability, proliferation, differentiation, and ECM production. In parallel, hMSCs can modulate their surrounding hydrogel. When the hMSCs start the production of ECM, they secrete matrix-altering proteins including extracellular proteases such as plasmin and matrix metalloproteinases (MMPs).[59–61] The secreted proteases could have a proteolytic effect on the hydrogel biodegradability. To look into this in further detail, hMSCs were cultured in a 25 mg mL^{-1} gel (20 mM) and incubated for 12 days, before the gel was disassembled by dilution in 1% TFA in water/acetonitrile (50/50 V/V), and the quantity of octapeptide present was determined using RP-HPLC. The TFA was used to ensure the denaturation of cell and serum proteases to stop any hydrolytic reactions at the desired time points. After 1 day of culture of hMSCs with serum, the hydrogel lost a significant quantity of hydrogel with only 38.3% ± 4.4% intact octapeptide remaining (Figure 12). The hydrogel was further degraded and/or eroded over time, with ~90% degraded after 6 days (9.1% ± 0.1% intact peptide) and almost completely degraded after 12 days, with only 1.2% ± 0.9% intact octapeptide remaining. To explore whether the observed loss of peptide hydrogel was catalyzed by proteases secreted by cells, hMSCs were cultured in the peptide hydrogel (25 mg mL^{-1}, 20 mM) using a serum-free media. After 1 day, the peptide was degraded significantly with only 39.7% ± 9.3% octapeptide remaining (Figure 12). Furthermore, hydrogel was degraded after incubation for longer times, with almost 80% of the octapeptide having degraded after 6 days (23.3% ± 0.1% intact peptide) and ~90% after 12 days (8.4% ± 1.4% intact peptide) (Figure 12). This result clearly shows that the cells exhibit an inherent proteolytic activity, as they hydrolyze the gel most likely by secreting proteases. To evaluate the hydrolytic effect of serum proteases on the peptide hydrogel, the cell-free gel was incubated with cell culture media containing 10% FBS over 12 days. After 1 day incubation, >60% of the peptide was degraded (36% ± 0.03% intact peptide). Longer incubation periods showed higher hydrolysis with 12.6% ± 0.2% and 5.3% ± 1.3% intact peptide remaining after 6 and 12 days, respectively. Swanekamp and co-workers have observed a similar degradability profile for the pleated β-sheet peptide L-Ac-$(FKFE)_2$-NH_2 when incubated with chymotrypsin, trypsin, and proteinase K over 5 days. The 0.5-mM peptide solution showed significant degradability with the three proteases with ~50% loss after 1 day and >95% hydrolysis after 5 days of incubation. Also, they observed that the 8-mM peptide hydrogel integrity was almost totally impaired after >4 h of incubation with 1 mg mL^{-1} chymotrypsin, indicating the breakdown of the hydrogel.[53]

The data presented here indicate that both serum and cells induce substantial hydrolytic breakdown of the peptide hydrogel, although the majority is likely to be due to simple erosion during the frequent media changes as there is also a considerable loss of octapeptide in the hydrogel with no serum or cells. Having said that, the FEFEFKFK octapeptide is formed of natural L-α-amino acids and is thus inherently vulnerable to hydrolysis by proteases present in the body. This design offers the potential use of such peptide hydrogels as delivery materials for cell therapies, as they would protect the cells once injected in vivo and act as an artificial ECM support for cell proliferation

and differentiation. As the cells go onto lay down their own ECM, the hydrogel will degrade and be processed by proteases and safely excreted.

Conclusion

Results from this study demonstrate that hMSCs can be incorporated homogeneously and proliferate within a 3D ionic-complementary peptide FEFEFKFK hydrogel. These cells were subsequently induced to commit into osteoblast cells simply via the addition of osteogenic culture medium. This was significant as it eliminates the prerequisite of adding any ECM biological cues. Once differentiated, these osteoblast cells were able to synthesize proteins such as Col-1, OCN, and ALP, which are all typically involved in the formation of bone. Moreover, differentiated cells supported within the hydrogel were able to mineralize, demonstrating the initial stages of bone formation. This work, therefore, exemplifies a simple and cost-effective biodegradable biomaterial that can be employed for the regeneration of hard tissues, such as alveolar bone. It requires no additional functionalization with, for example, ECM-isolated ligand sequences. Furthermore, it does not require any complex synthesis step, which is associated with arginine-rich peptides such as the RADA systems. This octapeptide system has the added potential of being a biodegradable injectable viscoelastic material in vivo or in situ, avoiding most of the post-surgical complications currently employed during bone grafting today.

Acknowledgements

The authors would like to thank the members of the Polymers & Peptides and the Biomaterials and Tissue Engineering Research Groups at UoM for their helpful discussions. All research data supporting this publication are directly available within this publication.

Declaration of conflicting interests

The author(s) declared no potential conflicts of interest with respect to the research, authorship, and/or publication of this article.

Funding

The author(s) disclosed receipt of the following financial support for the research, authorship, and/or publication of this article: This study was financially supported by CONACyT Mexico.

References

1. Feng X and McDonald JM. Disorders of bone remodeling. *Annu Rev Pathol* 2011; 6: 121–145.
2. Graves DT, Oates T and Garlet GP. Review of osteoimmunology and the host response in endodontic and periodontal lesions. *J Oral Microbiol*. Epub ahead of print 17 January 2011. DOI: 10.3402/jom.v3i0.5304.
3. Clarke B. Normal bone anatomy and physiology. *CJASN* 2008; 3(Suppl 3): S131–S139.
4. Perez-Chaparro PJ, Goncalves C, Figueiredo LC, et al. Newly identified pathogens associated with periodontitis: a systematic review. *J Dent Res* 2014; 93(9): 846–858.
5. Rogers GF and Greene AK. Autogenous bone graft: basic science and clinical implications. *J Craniofac Surg* 2012; 23(1): 323–327.
6. Roukis TS, Zgonis T and Tiernan B. Autologous platelet-rich plasma for wound and osseous healing: a review of the literature and commercially available products. *Adv Ther* 2006; 23(2): 218–237.
7. Giannoudis PV, Dinopoulos H and Tsiridis E. Bone substitutes: an update. *Injury* 2005; 36(Suppl. 3): S20–S27.
8. Caplan AI. Adult mesenchymal stem cells for tissue engineering versus regenerative medicine. *J Cellular Physiol* 2007; 213(2): 341–347.
9. Forbes SJ, Vig P, Poulsom R, et al. Adult stem cell plasticity: new pathways of tissue regeneration become visible. *Clin Sci (Lond)* 2002; 103(4): 355–369.
10. Engler AJ, Sen S, Sweeney HL, et al. Matrix elasticity directs stem cell lineage specification. *Cell* 2006; 126(4): 677–689.
11. Saha K, Keung AJ, Irwin EF, et al. Substrate modulus directs neural stem cell behavior. *Biophys J* 2008; 95(9): 4426–4438.
12. Arany PR, Cho A, Hunt TD, et al. Photoactivation of endogenous latent transforming growth factor-beta1 directs dental stem cell differentiation for regeneration. *Sci Trans Med* 2014; 6(238): 238ra69.
13. Chen J, Shi ZD, Ji X, et al. Enhanced osteogenesis of human mesenchymal stem cells by periodic heat shock in self-assembling peptide hydrogel. *Tissue Eng Part A* 2013; 19(5–6): 716–728.
14. Sila-Asna M, Bunyaratvej A, Maeda S, et al. Osteoblast differentiation and bone formation gene expression in strontium-inducing bone marrow mesenchymal stem cell. *Kobe J Med Sci* 2007; 53(1–2): 25–35.
15. Hsiong SX, Carampin P, Kong HJ, et al. Differentiation stage alters matrix control of stem cells. *J Biomed Mater Res Part A* 2008; 85(1): 145–156.
16. Tibbitt MW and Anseth KS. Hydrogels as extracellular matrix mimics for 3D cell culture. *Biotechnol Bioeng* 2009; 103(4): 655–663.
17. Gandavarapu NR, Alge DL and Anseth KS. Osteogenic differentiation of human mesenchymal stem cells on alpha5 integrin binding peptide hydrogels is dependent on substrate elasticity. *Biomater Sci* 2014; 2(3): 352–361.
18. Dasgupta A, Mondal JH and Das D. Peptide hydrogels. *RSC Adv* 2013; 3(24): 9117.
19. Mujeeb A, Miller AF, Saiani A, et al. Self-assembled octapeptide scaffolds for in vitro chondrocyte culture. *Acta Biomater* 2013; 9(1): 4609–4617.
20. Boothroyd S, Saiani A and Miller AF. Controlling network topology and mechanical properties of co-assembling peptide hydrogels. *Biopolymers* 2014; 101(6): 669–680.
21. Yan C and Pochan DJ. Rheological properties of peptide-based hydrogels for biomedical and other applications. *Chem Soc Rev* 2010; 39(9): 3528–3540.
22. Guilbaud JB, Rochas C, Miller AF, et al. Effect of enzyme concentration of the morphology and properties of enzymatically triggered peptide hydrogels. *Biomacromolecules* 2013; 14(5): 1403–1411.

23. Nune M, Kumaraswamy P, Krishnan UM, et al. Self-assembling peptide nanofibrous scaffolds for tissue engineering: novel approaches and strategies for effective functional regeneration. *Curr Protein Peptide Sci* 2013; 14(1): 70–84.
24. Anderson JM, Vines JB, Patterson JL, et al. Osteogenic differentiation of human mesenchymal stem cells synergistically enhanced by biomimetic peptide amphiphiles combined with conditioned medium. *Acta Biomater* 2011; 7(2): 675–682.
25. Tcacencu I, Karlstrom E, Cedervall J, et al. Transplanted human bone marrow mesenchymal stem cells seeded onto peptide hydrogel decrease alveolar bone loss. *BioRes Open Access* 2012; 1(5): 215–221.
26. Matsumoto T, Tadokoro M, Hattori K, et al. Osteogenic differentiation of mesenchymal stem cells/polymer composites with HA in vitro. *Biocer Dev Appl* 2011; 1: 1–4.
27. Saiani A, Mohammed A, Frielinghaus H, et al. Self-assembly and gelation properties of alpha-helix versus beta-sheet forming peptides. *Soft Matter* 2009; 5(1): 193–202.
28. Gough JE, Saiani A and Miller AF. Peptide hydrogels: mimicking the extracellular matrix. *Bioins Biomim Nanobiomater* 2012; 1(1): 4–12.
29. Diaz LAC, Gough J, Saiani A, et al. Human osteoblasts within soft peptide hydrogels promote mineralisation in vitro. *J Tissue Eng* 2014; 5: 2041731414539344.
30. Benoit DS, Durney AR and Anseth KS. The effect of heparin-functionalized PEG hydrogels on three-dimensional human mesenchymal stem cell osteogenic differentiation. *Biomaterials* 2007; 28(1): 66–77.
31. Jilka RL, Weinstein RS, Parfitt AM, et al. Quantifying osteoblast and osteocyte apoptosis: challenges and rewards. *J Bone Miner Res* 2007; 22(10): 1492–1501.
32. Catelas I, Sese N, Wu BM, et al. Human mesenchymal stem cell proliferation and osteogenic differentiation in fibrin gels in vitro. *Tissue Eng* 2006; 12(8): 2385–2396.
33. Xu J, Wang W, Ludeman M, et al. Chondrogenic differentiation of human mesenchymal stem cells in three-dimensional alginate gels. *Tissue Eng Part A* 2008; 14(5): 667–680.
34. Wiesmann A, Buhring HJ, Mentrup C, et al. Decreased CD90 expression in human mesenchymal stem cells by applying mechanical stimulation. *Head Face Med* 2006; 2: 8.
35. Kortesidis A, Zannettino A, Isenmann S, et al. Stromal-derived factor-1 promotes the growth, survival, and development of human bone marrow stromal stem cells. *Blood* 2005; 105(10): 3793–3801.
36. Lee HJ, Choi BH, Min BH, et al. Changes in surface markers of human mesenchymal stem cells during the chondrogenic differentiation and dedifferentiation processes in vitro. *Arthritis Rheum* 2009; 60(8): 2325–2332.
37. George J, Kuboki Y and Miyata T. Differentiation of mesenchymal stem cells into osteoblasts on honeycomb collagen scaffolds. *Biotechnol Bioeng* 2006; 95(3): 404–411.
38. Gershovich JG, Dahlin RL, Kasper FK, et al. Enhanced osteogenesis in cocultures with human mesenchymal stem cells and endothelial cells on polymeric microfiber scaffolds. *Tissue Eng Part A* 2013; 19(23–24): 2565–2576.
39. Birmingham E, Niebur GL, McHugh PE, et al. Osteogenic differentiation of mesenchymal stem cells is regulated by osteocyte and osteoblast cells in a simplified bone niche. *Eur Cell Mater* 2012; 23: 13–27.
40. Keskar V, Marion NW, Mao JJ, et al. In vitro evaluation of macroporous hydrogels to facilitate stem cell infiltration, growth, and mineralization. *Tissue Eng Part A* 2009; 15(7): 1695–1707.
41. Kim J, Hefferan TE, Yaszemski MJ, et al. Potential of hydrogels based on poly(ethylene glycol) and sebacic acid as orthopedic tissue engineering scaffolds. *Tissue Eng Part A* 2009; 15(8): 2299–2307.
42. Sapir-Koren R and Livshits G. Bone mineralization and regulation of phosphate homeostasis. *IBMS BoneKEy* 2011; 8(6): 286–300.
43. Nudelman F, Pieterse K, George A, et al. The role of collagen in bone apatite formation in the presence of hydroxyapatite nucleation inhibitors. *Nature Mater* 2010; 9(12): 1004–1009.
44. Gajjeraman S, Narayanan K, Hao J, et al. Matrix macromolecules in hard tissues control the nucleation and hierarchical assembly of hydroxyapatite. *J Biol Chem* 2007; 282(2): 1193–1204.
45. Hamada K, Hirose M, Yamashita T, et al. Spatial distribution of mineralized bone matrix produced by marrow mesenchymal stem cells in self-assembling peptide hydrogel scaffold. *J Biomed Mater Res Part A* 2008; 84(1): 128–136.
46. Nuttelman CR, Benoit DS, Tripodi MC, et al. The effect of ethylene glycol methacrylate phosphate in PEG hydrogels on mineralization and viability of encapsulated hMSCs. *Biomaterials* 2006; 27(8): 1377–1386.
47. Elisseeff J. Hydrogels: structure starts to gel. *Nature Mater* 2008; 7(4): 271–273.
48. Amini AA and Nair LS. Injectable hydrogels for bone and cartilage repair. *Biomed Mater* 2012; 7(2): 024105.
49. Zheng X, Baker H, Hancock WS, et al. Proteomic analysis for the assessment of different lots of fetal bovine serum as a raw material for cell culture. Part IV. Application of proteomics to the manufacture of biological drugs. *Biotechnol Progr* 2006; 22(5): 1294–1300.
50. El-Fiqi A, Lee JH, Lee EJ, et al. Collagen hydrogels incorporated with surface-aminated mesoporous nanobioactive glass: improvement of physicochemical stability and mechanical properties is effective for hard tissue engineering. *Acta Biomater* 2013; 9(12): 9508–9521.
51. Shin H, Jo S and Mikos AG. Biomimetic materials for tissue engineering. *Biomaterials* 2003; 24(24): 4353–4364.
52. Nicodemus GD and Bryant SJ. Cell encapsulation in biodegradable hydrogels for tissue engineering applications. *Tissue Eng Part B Rev* 2008; 14(2): 149–165.
53. Swanekamp RJ, Welch JJ and Nilsson BL. Proteolytic stability of amphipathic peptide hydrogels composed of self-assembled pleated beta-sheet or coassembled rippled beta-sheet fibrils. *Chem Commun* 2014; 50(70): 10133–10136.
54. Banerjee A, Arha M, Choudhary S, et al. The influence of hydrogel modulus on the proliferation and differentiation of

encapsulated neural stem cells. *Biomaterials* 2009; 30(27): 4695–4699.
55. Wang LS, Chung JE, Chan PP, et al. Injectable biodegradable hydrogels with tunable mechanical properties for the stimulation of neurogenesic differentiation of human mesenchymal stem cells in 3D culture. *Biomaterials* 2010; 31(6): 1148–1157.
56. Wen JH, Vincent LG, Fuhrmann A, et al. Interplay of matrix stiffness and protein tethering in stem cell differentiation. *Nature Mater* 2014; 13: 979–987.
57. Beniash E, Hartgerink JD, Storrie H, et al. Self-assembling peptide amphiphile nanofiber matrices for cell entrapment. *Acta Biomater* 2005; 1(4): 387–397.
58. Cunha C, Panseri S, Villa O, et al. 3D culture of adult mouse neural stem cells within functionalized self-assembling peptide scaffolds. *Int J Nanomed* 2011; 6: 943–955.
59. Kasper G, Dankert N, Tuischer J, et al. Mesenchymal stem cells regulate angiogenesis according to their mechanical environment. *Stem Cells* 2007; 25(4): 903–910.
60. Lozito TP, Taboas JM, Kuo CK, et al. Mesenchymal stem cell modification of endothelial matrix regulates their vascular differentiation. *J Cell Biochem* 2009; 107(4): 706–713.
61. Lozito TP, Jackson WM, Nesti LJ, et al. Human mesenchymal stem cells generate a distinct pericellular zone of MMP activities via binding of MMPs and secretion of high levels of TIMPs. *Matrix Biol* 2014; 34: 132–143.